

BREAST CONTOUR DETECTION WITH SHAPE PRIORS

Ricardo Sousa*, Jaime S. Cardoso†, J. F. Pinto da Costa‡, M. J. Cardoso§

ABSTRACT

Breast cancer conservative treatment (BCCT) is considered the gold standard of breast cancer treatment. However, aesthetic results are heterogeneous and difficult to evaluate in a standardised way. The limited reproducibility of subjective aesthetic evaluation in BCCT forced the research on objective methods. A recent computer system was developed to objectively and automatically evaluate the aesthetic result of BCCT. In this system, the detection of the breast contour on the digital photograph of the patient is necessary to extract the features subsequently used in the evaluation process.

In this paper we extend an algorithm based on the shortest path on a graph to detect automatically the breast contour. The advantage of graph algorithms is that they are guaranteed to find the global optimum of the problem; the difficulty is that they make it hard to enforce shape constraints. We define and compare different techniques to introduce the a priori knowledge of the mammary contour. Experimental results show that the proposed techniques consistently outperform the base method.

Index Terms— Biomedical image processing, medical expert systems, image analysis, shortest path, shape prior modeling.

1. INTRODUCTION

The oncological outcome of Breast Cancer Conservative Treatment (BCCT) is equivalent to mastectomy in terms of overall survival. The absence of a standardised tool for aesthetic evaluation of this kind of treatment limits, however, the applicability of any comparative analysis of cosmetic outcome. Subjective methods usually evaluate a patient's appearance by one or several observers. However, results of subjective evaluation show only a modest inter-observer agreement, even when performed by expert observers [1]. Objective methods, using measurements taken directly from the patient or from photographs, increase the reproducibility of the assessment.

The BCCT.core software was developed to provide an objective and automatic evaluation of the aesthetical result, not only based on asymmetries, but also based on other parameters (surgical scar appearance and skin colour difference) extracted from patients' photographs. This objective score was translated into a result according to Harris scale: excellent, good, fair, or poor. The aim was to develop a reproducible and widely available methodology for the evaluation of aesthetic results in BCCT, enabling effective comparison of outcome between centers [2].

*INESC Porto, Faculdade de Ciências, Universidade do Porto, Portugal email: rsousa@inescporto.pt

†INESC Porto, Faculdade de Engenharia, Universidade do Porto, Portugal email: jaime.cardoso@inescporto.pt

‡Faculdade de Ciências, Universidade do Porto, Portugal email: jpcosta@fc.up.pt

§INESC Porto, Faculdade de Medicina, Universidade do Porto, Portugal email: mjcard@med.up.pt

This work was partially funded by Fundação para a Ciência e a Tecnologia (FCT) - Portugal through project PTDC/EIA/64914/2006.

The use of BCCT.core to assess the overall aesthetic result entails the automatic extraction of several features from the photograph of the patient (see Figure 1a for a typical photograph), capturing some of the factors considered to have impact on the overall cosmetic result: breast asymmetry, skin colour changes due to the radiotherapy treatment, and surgical scar visibility [2]. In order to extract the identified relevant features from the image, the detection of the breast contour is necessary. In [3] the authors describe a *semi-automatic* method for the detection of the breast contour which the user has to *manually* identify the two endpoints of the breast contour, with the algorithm automatically finding the contour in-between. Subsequently the user input was eliminated by automatically detecting the endpoints of the breast contour [4].

Nevertheless, the results for the breast contour detection, both for manually and automatically placed endpoints, are not always satisfactory. Occasionally, the method outputs an anatomically unlikely breast contour. This is especially true on women with small breasts (leading to weak contours)—for which the method may propose a straight line for the breast contour—, or on low-quality images, when the methods may be fooled to follow other anatomic parts, like the edge of the torso. Here, we improve on [3, 4] by incorporating shape information on the contour detection algorithm. The shape constraint makes the contour detection algorithm more robust to avoid distracting edges, and the graph algorithm guarantees that the best solution is found.

Before presenting the proposed approach, and for completeness, we recover the framework for breast contour detection between two *known endpoints* of [3]. Then, in Section 3, we describe parametric and non-parametric alternatives to define our a priori knowledge about the shape of the breast and incorporate that knowledge in the shortest path algorithm. Next, we provide a thorough evaluation of the performance of the proposed method against manually-outlined breast contours. Examples are provided and a performance analysis is conducted in Section 4. In Section 5, we conclude the paper.

2. PREVIOUS WORK

In the previous work [3], the breast contour detection with known endpoints was solved by finding the minimum cost path between the source and the destination endpoints in a graph whose nodes correspond to the pixels in the image and edges connect neighbouring pixels. The weight function on the edges was defined so that the shortest path corresponds to a path that maximises the amount of edge strength in the image along the contour. The weight of the edge connecting 4-neighbour pixels p and q was expressed as an exponential law

$$\hat{f}(g) = \alpha \exp(\beta (255 - g)) + \gamma, \quad (1)$$

with $\alpha, \beta, \gamma \in \mathbb{R}$ and g is the average of the gradient computed on the two incident pixels. For 8-neighbour pixels the weight was set to $\sqrt{2}$ times that value. The parameters α, β, γ were experimentally tuned, yielding $\alpha = 0.15, \beta = 0.0208, \gamma = 1.85$. Having the problem of contour detection been formulated as a shortest path problem,

a number of algorithms are available in the graph theory literature to find the optimal solution, such as the Dijkstra’s algorithm [5].

To enforce shape constraints, deformable templates are often used. Prototype-based deformable templates are usually constructed from a set of training examples. Then principal component analysis is applied to define an average template shape and modes of variation [6, 7, 8]. Unfortunately, when graph algorithms are used, the cost function is influenced by only two consecutive pixels at a time. More pixels would be needed to encode shape information. Nevertheless, graph algorithms have the advantage over gradient descent—typical on active contours—in that they recover the optimal solution and do not get trapped in local minimal. Therefore, in the following, we proposed different approaches to encode the a priori shape knowledge in the graph design.

3. PRIOR SHAPE MODELLING

When localising the breast contour, prior knowledge is very helpful. To incorporate this into the shortest path process, we consider different alternatives to modify the weight function of the graph, reflecting our knowledge of the shape. The weight function will be modified by a term measuring the shape probability. The shortest path problem is then formulated on this modified weighted graph. The key advantage of this approach is that the shortest path computation is left unchanged and hence is efficient and discovers the optimal solution. Yet, the challenge is now to construct a good description of the space of breast shapes in the graph model.

3.1. Parametric prior

Standard analytical parametric models encode the geometric shape with a small number of parameters. The typical round or tear drop shape of a breast suggests that a conic section is a good approximation to the breast contour. Note however that the breast contour may be severely deformed after the surgical intervention, in relation to its typical shape. This justifies that the regression by a conic section would not be flexible enough to, by itself, yield the final breast contour. However, that same limitation can be used in our benefit. Because it is more constrained, it can be robustly estimated from a noisy, small set of data. We consider the output of this regression as a priori knowledge about the shape and size of the breast. One may think this as empirical prior—prior, because the type of admissible curves are based in our a priori knowledge; empirical, because the parameters are estimated from the data itself. Note that we perform the regression on the patient to assess, and do not try to arrive at an average breast contour from a train set of manually outlined breast contours. That is because the high variability of contours in size and shape would render the average breast ineffective.

Next, to add this prior shape information into the contour detection process, the Euclidean distance map was used as a representation of the regression curve. We represent the curve \mathcal{C} by its Euclidean distance transform map Φ , where $\Phi(x, y)$ is the Euclidean distance to the closest point of \mathcal{C} . Hence the Euclidean distance transformation creates an image where the value of each pixel is the distance from this pixel to the nearest pixel belonging to the curve \mathcal{C} . Note that by definition $\mathcal{C} = \{(x, y) | \Phi(x, y) = 0\}$.

The design of the weight function has previously included only the gradient information. We can now generalise the expression of the weights by including a component penalising pixels with a high Euclidean distance value. The rationale supporting this decision is that the contour points will, with high probability, be close to the regression curve and the probability of belonging to the breast contour

decays with the increase of the Euclidean distance. An exponential increase on the weights of the edges was modelled as

$$\hat{f}(g, d) = \alpha \exp(\beta_1 (255 - g) + \beta_2 d) + \gamma, \quad (2)$$

with $\alpha, \beta_1, \beta_2, \gamma \in \mathbb{R}$ and d the average of the Euclidean distance values computed on the two incident pixels.

We considered three alternatives for curve \mathcal{C} : parabola, cubic and ellipse.

3.1.1. Parabola

To obtain the parabola best fitting the data, a constrained least square regression was performed on the edge points (x_i, y_i) , $i = 1, \dots, N$ inside the vertical strip defined by the two known breast contour end-points, (x_1, y_1) and (x_N, y_N) .

Imposing that the parabola has to contain the two known end-points of the breast contour, the regression problem results as

$$\begin{aligned} \min_{a_1, a_2, a_3} \quad & \sum_{i=1}^N (y_i - (a_1 x_i^2 + a_2 x_i + a_3))^2 \\ \text{s.t.} \quad & a_1 x_1^2 + a_2 x_1 + a_3 = y_1 \\ & a_1 x_N^2 + a_2 x_N + a_3 = y_N \end{aligned}$$

Positioning one of the two endpoints (say (x_1, y_1)) at the origin with a simple translation, the first constraint yields immediately $a_3 = 0$ and the second constraint produces $a_2 = \frac{y_N}{x_N} - a_1 x_N$. Solving the minimisation problem on the single parameter a_1 produces the optimal value $a_1 = \frac{\sum_{i=1}^N (y_i x_i (x_i - x_N) + \frac{y_N}{x_N} x_i)}{\sum_{i=1}^N x_i^2 (x_i - x_N)^2}$. Finally, the translation was reversed to obtain the curve on the original space.

The potentially insufficient flexibility of a parabola (constrained by two points), led us to assess a cubic regression; experimental results contradicted our initial conviction. Consequently, we have only included results for the second-degree polynomial regression in subsequent tables.

3.1.2. Ellipse

The typical shape of a breast also suggests trying to find the ellipse that fits best (in least-squares sense) to the edge points [9]. Imposing the same assumptions as in the parabola fitting, we obtained the best ellipse fitting the data and containing the two endpoints. Finally, only the elliptic arc below the cord connecting the two endpoints was considered as the a priori curve.

3.2. Non-parametric prior

A difficulty with the parametric approach just presented is that the quality of the final contour is highly correlated with the quality of the regression operation. In this section we consider non-parametric alternatives to impose the a priori knowledge. The first approach learns the shape prior from a set of known breast contours; the second simply tries to enforce our intuitive shape knowledge.

3.2.1. Mask prior

Supposing that we have a training set $\mathcal{C} = \{C_i | i = 1, 2, \dots, M\}$ of M registered breast contours, manually outlined, we propose to construct a nonparametric breast shape prior by defining an admissible breast contour region. Considering the breast contours as closed curves, we defined the difference between the reunion and the intersection of all breast contour regions:

$$\mathcal{R} = \cup_{i=1}^M \mathcal{C}_i - \cap_{i=1}^M \mathcal{C}_i$$

Region \mathcal{R} is the smallest simply connected region that contains all breast contours on the training set. If the training set is representative of the population—it was drawn from the underlying breast shape and size distribution—, one expects that unseen breast contours will be found (almost) entirely inside the region \mathcal{R} .

The registration of the breast contours in the training set was achieved by setting, with a suitable transformation, one endpoint at $(0, 0)$ and the other in the $(1, 0)$ position. To accomplish that, we first position (x_1, y_1) at the origin by translating every contour point; next, every translated point, P' , is rotated by the rotation matrix \mathcal{R} as given in Equation (3), where θ is the angle between endpoints P_1 and P_N . Finally, the positioning of P_N in $(1, 0)$ is completed by scaling every transformed point (x'_i, y'_i) by the scale matrix \mathcal{S} (see also Equation (3)), where x''_i are all points of $P'' = \mathcal{R} * P'$.

$$\mathcal{R} = \begin{bmatrix} \cos(\theta) & -\sin(\theta) \\ \sin(\theta) & \cos(\theta) \end{bmatrix}, \quad \mathcal{S} = \begin{bmatrix} 1/x''_N & 0 \\ 0 & 1/y''_N \end{bmatrix} \quad (3)$$

The incorporation of this prior information into the breast contour detection process followed the approach used on the parametric case. The region \mathcal{R} is represented by its Euclidean distance map, where the distance from each pixel is computed to the nearest pixel belonging to the region \mathcal{R} . The process finalises with the same weight function, as given in Equation (2).

Fig. 1 illustrates the Euclidean distance maps obtained with the different models for the left breast of Patient #59. Black pixels rep-

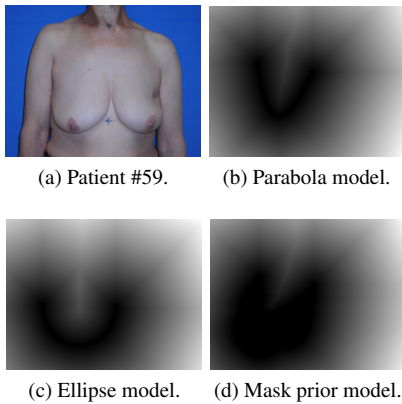


Fig. 1: Euclidean distance maps for the left breast of Patient #59.

resent pixels with high probability of belonging to the breast contour taking into consideration only our prior knowledge about the breast shape.

3.2.2. Unimodal model

Intuitively, the breast contour is monotonically decreasing from one endpoint down to a minimum point, located approximately in the middle position, and from there it monotonically increases up to the other endpoint.

This simple perception about the shape of the breast can be enforced by running the shortest path algorithm in a phased process, instead of directly finding the path between the two given endpoints. To favour a first descending path, we find the shortest path between the external endpoint and a point located at the same column as the internal endpoint, but y_{Gap} rows below. We set y_{Gap} to twice the x difference between the two endpoints (and therefore relatively robust to the size of the patient in the image). In the second step of the

process, we compute a second shortest path between the point of the first path at the x -middle position and the internal endpoint.

Note that, in spite of the name, the unimodal does capture any fluctuation or irregularity in the evolution of contour, as it retains the flexibility of the shortest path process. Secondly, although the auxiliary point is positioned only twice width of the breast below the endpoint, the contour can, naturally, go below that point—the actual shape is again captured by the shortest path. Finally, observe that the unimodal model relies only in Equation 1 to construct the weighted graph.

4. RESULTS

The methodology proposed in this paper was assessed on a set of 190 photographs. All patients were treated with conservative breast surgery, with or without auxiliary surgery, and whole breast radiotherapy, with treatment completed at least one year before the onset of the study. A mark was made on the skin at the suprasternal notch and at the mid line 25 cm below the first mark (see Figure 1a). These two marks create a correspondence between pixels measured on the photograph and the length in centimetres on the patient.

In order to investigate the possibility of defining an automated method of detecting the breast contour, a set of patients with known breast contour was required. Since, ideally, the automated method should correlate coherently with human assessment, eight different observers were asked to manually draw the contours. A software tool was developed specifically to assist on this job [2].

Before applying the proposed algorithm, each image was down-sized to a constant width of 768 pixels, while keeping the aspect ratio. This improves the computational performance, without degrading the quality of the final result.

To find the best parameterization of each model, we performed a “grid-search” on the parameter space using cross-validation on a training set (40% of the data). The performance was then assessed on the test set (60% of the data). Instead of a visual and subjective evaluation as employed in [3], we conducted an objective evaluation based on the Hausdorff and the average distances to compare two contours. The Hausdorff distance is defined as the “maximum distance of a set to the nearest point in the other set”. Roughly speaking, it captures the maximum separation between the manual and the automatic contours. Table 1 summarises the results for the average distance on the test set, whereas Table 2 summarises the Hausdorff results. Figure 2 shows some of results for Patient #59.

Method		Error (cm)		
		mean	std. dev.	max.
Base model	left breast	1.46	2.74	10.82
	right breast	1.45	2.74	9.08
Parabola	left breast	1.17	1.43	6.87
	right breast	1.09	1.24	8.11
Ellipse	left breast	1.54	1.58	8.01
	right breast	1.21	1.22	5.69
Mask	left breast	0.25	0.61	5.52
	right breast	0.27	0.68	4.91
Unimodal	left breast	0.24	0.61	6.23
	right breast	0.30	0.88	8.81

Table 1: Average distance in the position of the breast contour.

The main assertion concerns the superiority of models with prior over the base model: not only their mean error is lower but also their performance ability tends to be less variable. A second outcome

Method		Error (cm)		
		mean	std. dev.	max.
Base model	left breast	4.52	6.27	23.80
	right breast	4.52	6.45	23.08
Parabola	left breast	4.49	4.02	18.33
	right breast	4.19	3.27	21.45
Ellipse	left breast	4.14	3.32	19.91
	right breast	4.65	3.66	16.01
Mask	left breast	1.81	1.78	14.04
	right breast	1.78	1.87	13.22
Unimodal	left breast	1.90	2.05	17.82
	right breast	1.98	2.45	21.44

Table 2: Hausdorff distance in the position of the breast contour.

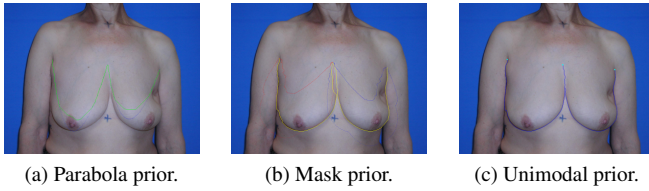


Fig. 2: Results of contour detection for Patient #59.

of this study is the superiority of the non-parametric models over the other parametric ones. This conclusion may embody the greater robustness of the former against adverse conditions on the capture process of the images. Note that the parametric models are based on a regression on the patient image under evaluation; as such, do not benefit from the knowledge extracted from a set of known contours.

In a last set of experiments, the quality of the breast contour tracking algorithms was assessed with the endpoints automatically positioned using the procedure proposed in [4]. The procedure requires the detection of the trunk contour, which is based on the concept of strong or stable contours, also introduced in that work.

Having already established the superiority of the non-parametric models, only the results for these are presented in Table 3 and Table 4. While with manually placed endpoint, it seems that there are

Method		Error (cm)		
		mean	std. dev.	max.
Mask	left breast	1.01	2.76	14.70
	right breast	0.79	2.20	12.45
Unimodal	left breast	0.56	1.52	9.64
	right breast	0.50	1.44	10.67

Table 3: Average distance in the position of the breast contour, with endpoints automatically positioned.

Method		Error (cm)		
		mean	std. dev.	max.
Mask	left breast	3.42	5.35	29.20
	right breast	2.98	4.40	21.55
Unimodal	left breast	3.25	4.46	21.68
	right breast	2.82	4.13	24.02

Table 4: Hausdorff distance in the position of the breast contour, with endpoints automatically positioned.

no significant differences between the two parametric models, the unimodal model has a better resilience performance against possible failures on the endpoints' position. The natural degradation, observed on the performance with automatically placed endpoints, is less pronounced with this model than with the mask based model.

5. CONCLUSION

We have described in this paper a method for breast contour detection with shape constraints formulated as a shortest path algorithm problem. Diverse strategies were studied to incorporate shape a priori knowledge. Our approaches retain the benefits of efficiency and certainty to recover the global optimum, familiar attributes of the shortest path algorithms. On the experimental study the inclusion of shape prior information increased the quality of the contours detected. The medical interest of the proposed method is to provide a totally automated tool to assure an objective analysis of the aesthetical result of BCCT.

6. REFERENCES

- [1] M. J. Cardoso, A. C. Santos, Jaime S. Cardoso, H. Barros, and M. C. Oliveira, "Choosing observers for evaluation of aesthetic results in breast cancer conservative treatment," *International Journal of Radiation Oncology, Biology and Physics*, vol. 61, pp. 879–881, 2005.
- [2] Jaime S. Cardoso and Maria J. Cardoso, "Towards an intelligent medical system for the aesthetic evaluation of breast cancer conservative treatment," *Artificial Intelligence in Medicine*, vol. 40, pp. 115–126, 2007.
- [3] Jaime S. Cardoso and M. J. Cardoso, "Breast contour detection for the aesthetic evaluation of breast cancer conservative treatment," in *Springer Lecture Notes in Computer Science, Advances in Soft Computing 45, Computer Recognition Systems 2 – CORES 2007: 5th International Conference on Computer Recognition Systems*, October 2007, pp. 518–525.
- [4] Jaime S. Cardoso, Luis F. Teixeira, and M. J. Cardoso, "Automatic breast contour detection in digital photographs," in *International Conference on Health Informatics (HEALTH-INF2008)*, 2008, vol. 2, pp. 91–98.
- [5] E. W. Dijkstra, "A note on two problems in connexion with graphs," *Numerische Mathematik*, vol. 1, pp. 269–271, 1959.
- [6] A. Tsai, A. Yezzi, W. Wells, C. Tempny, D. Tucker, A. Fan, W. E. Grimson, and A. Willsky, "A shape-based approach to the segmentation of medical imagery using level sets," *IEEE Transactions on Medical Imaging*, vol. 22, pp. 137–154, 2003.
- [7] Igor Dydenko, Fadi Jamal, Olivier Bernard, Jan D'Hooge, Isabelle E. Magnin, and Denis Friboulet, "A level set framework with a shape and motion prior for segmentation and region tracking in echocardiography," *Medical Image Analysis*, vol. 10, no. 2, pp. 162–177, April 2006.
- [8] P. Yan and A. A. Kassim, "Medical image segmentation using minimal path deformable models with implicit shape priors," *IEEE Transactions on Information Technology in Biomedicine*, vol. 10, pp. 677–684, 2006.
- [9] Andrew Fitzgibbon, Maurizio Pilu, and Robert B. Fisher, "Direct least square fitting of ellipses," *IEEE Transactions on Pattern Analysis and Machine Intelligence*, vol. 21, no. 5, pp. 476–480, 1999.